

RESEARCH

Open Access



Inhibition of IL-6 trans-signaling promotes post-stroke functional recovery in a sex and dose-dependent manner

Cassandra Hall^{1†}, Dustin T. Nguyen^{1†}, Kate Mendoza¹, Chunfeng Tan¹ and Anjali Chauhan^{1*}

Abstract

Introduction Elevated circulating IL-6 levels are associated with poorer outcomes after stroke, and increased serum IL-6 levels are linked to a higher risk of stroke. IL-6 binds to soluble IL-6 receptors (sIL-6R) and subsequently to ubiquitously expressed gp130, initiating proinflammatory trans-signaling. This study tested the hypothesis that inhibiting IL-6 trans-signaling by administering soluble (s) gp130 improves long-term functional outcomes in young mice after stroke.

Methods Recombinant mouse gp130Fc chimera (sgp130) was administered one hour after middle cerebral artery occlusion (MCAO) followed by twice-weekly administration for 2 weeks in mice (8–15 weeks old). Behavioral assessments were done on days 7 and 28 post-MCAO for chronic studies. Flow cytometry was performed on days 3 (blood) and 7 (spleen and brain) to assess IL-6, mIL-6R, and phosphorylated STAT3 expression.

Results Improved long-term functional outcomes were observed in male, but not female mice. To investigate the differential response in females, ELISA analyses revealed that plasma IL-6 levels increased in both sexes after MCAO, with a more pronounced induction in females. Additionally, circulating sIL-6R levels were significantly higher in females compared to males ($p < 0.05$) at 24 h post-MCAO. Administering a higher dose of sgp130 (1 mg/kg) to females improved long-term functional outcomes, suggesting that a higher dose is needed to inhibit IL-6 trans-signaling in females effectively. Mechanistically, sgp130 treatment reduced phosphorylated STAT3 expression in brain F4/80 macrophages and increased the expression of mIL-6R on splenic immune cells at day 7 post-MCAO in both sexes.

Conclusion These findings demonstrate that inhibition of IL-6 trans-signaling with gp130Fc improves long-term functional outcomes in both male and female mice, albeit in a dose-dependent manner. This study provides novel insights into potential therapeutic strategies targeting IL-6 signaling pathways following stroke.

Keywords IL-6, Trans-signaling, sgp130, Stroke, Sex-difference

[†]Cassandra Hall and Dustin T. Nguyen shared first authors.

*Correspondence:

Anjali Chauhan

anjali.chauhan@uth.tmc.edu

¹Department of Neurology, University of Texas McGovern Medical School at Houston, Houston, TX, USA



Introduction

Interleukin-6 (IL-6) is a cytokine secreted by multiple cell types, including microglia, macrophages, astrocytes, monocytes, fibroblasts, endothelial cells, mast cells, keratinocytes, and T cells [1]. IL-6 plays a pivotal role in the immune response and is involved in several inflammatory conditions, including ischemic stroke [2, 3]. IL-6 signaling occurs through two main pathways: classical signaling, which is anti-inflammatory, and trans-signaling, which is pro-inflammatory. In classical signaling, IL-6 binds directly to membrane-bound IL-6 receptors (mIL-6R) already complexed with gp130 [4, 5]. This pathway is restricted to cells expressing mIL-6R, such as hepatocytes, neutrophils, monocytes, macrophages, and some lymphocytes, limiting the number of cells that can engage in classical signaling [6]. In contrast, IL-6 trans-signaling occurs when IL-6 binds to soluble IL-6 receptor (sIL-6R). The IL-6/sIL-6R complex then binds to membrane (m)-bound gp130 [4, 5, 7]. Because gp130 is ubiquitously expressed, trans-signaling can occur in virtually any cell type, broadening the potential inflammatory responses mediated by IL-6. Therefore, selectively inhibiting IL-6 trans-signaling represents a promising therapeutic strategy for inflammatory conditions, aiming to mitigate excessive immune responses while preserving the beneficial aspects of IL-6 classical signaling.

The effects of manipulating IL-6 signaling have been extensively studied in numerous stroke investigations [8]. IL-6 is recognized as an early and chronic phase-inflammatory mediator, yet it also plays a role as a neurotrophic mediator [9]. Importantly, the effects of IL-6 within the brain may differ from those in peripheral tissues. For instance, locally produced IL-6 in the brain has been shown to promote angiogenesis post-stroke [10], and intracerebroventricular administration of IL-6 was neuroprotective in a rat model of permanent focal cerebral ischemia [11], suggesting a beneficial role of enhancing IL-6 specifically in the brain. However, elevated serum levels of IL-6 have been associated with larger infarct sizes and poorer outcomes in stroke patients [2, 3]. Therefore, targeting peripheral IL-6 while preserving beneficial central IL-6 effects may represent a therapeutic approach to improve stroke outcomes.

Selective blockade of IL-6 trans-signaling by soluble (s) gp130 has demonstrated protective effects against transverse aortic constriction-induced ventricular remodeling in young mice, reducing ventricular fibrosis, immune cell infiltration, and oxidative stress [12]. Additionally, sgp130 treatment decreases endothelial activation and intimal smooth muscle cell infiltration, thereby reducing monocyte recruitment and slowing atherosclerotic plaque progression [13]. Intracerebroventricular (ICV) administration of sgp130 has also attenuated LPS-induced

sickness behavior in adult and aged mice [14, 15], highlighting its efficacy across various disease models.

Although ischemic stroke primarily affects older adults, its incidence among young adults has been increasing globally [16–19]. While risk factors in younger patients often overlap with those in older patients, behaviors such as low physical activity, excessive alcohol consumption, and smoking contribute disproportionately to ischemic strokes in young adults. Therefore, it is critical to test therapies in younger patient populations. Consequently, we hypothesized that inhibiting IL-6 trans-signaling would enhance long-term functional outcomes after stroke in young mice. This study aimed to evaluate the enduring benefits of IL-6 trans-signaling inhibition by sgp130 and to investigate the underlying mechanisms influencing stroke-induced functional outcomes.

Materials and methods

Animals

Young adult male and female mice (8–15 weeks) were used for this study and were group housed in a pathogen-free facility with access to food and water *ad libitum*. All animals were group housed in Tecniplast individually ventilated cage racks, fed a commercially available irradiated, balanced mouse diet (no. 5058, LabDiet, St Louis, MO), and provided corncob bedding. Rooms were maintained at 21–24°C and under a 12:12 h light: dark cycle. Animal procedures were performed at an Association for Assessment and Accreditation of Laboratory Animal Care (AAALAC) accredited facility and were approved by the Animal Welfare Committee at the University of Texas Health Science Center in Houston, TX, USA. All the surgeries and behavioral testing were conducted between 6 and 9 AM by an investigator blinded to treatment.

Middle cerebral artery occlusion (MCAO)

Transient focal ischemia was induced under isoflurane anesthesia in young for 60 min by occlusion of the right middle cerebral artery [20]. Body temperature was maintained at 37.0 ± 1.0 °C throughout the surgery by an automated temperature control feedback system (TC1000, mouse, CWE Inc., USA). A midline ventral neck incision was made, and unilateral MCAO was performed by inserting a Doccol monofilament (Doccol Corp, Redlands, CA, USA, 602145PK10Re) through a right external carotid artery into the internal carotid artery. Cerebral blood flow (CBF) was measured by a Laser Doppler flowmeter (Moor Instruments Ltd., Devor, UK) to ensure occlusion (>80% from baseline) and later MCA recanalization. Animals were allowed to awaken from anesthesia during the intra-ischemic period to ensure behavioral deficits (turning). One hour after ischemia, animals were re-anesthetized, and reperfusion was established by the withdrawal of the monofilament. Animals were then

placed in a recovery cage and were euthanized either at 24 (efficacy study) or 72 h after reperfusion or 7 days post-MCAO (for assessment of mIL-6R, and mgp130). For chronic studies, mice were euthanized at day 15 (females only) or 30 post-MCAO. Sham controls underwent the same procedure except the monofilament was not introduced to occlude the middle cerebral artery. Animals were randomly assigned to stroke and sham surgery groups and housed in recovery cages for two hours after surgery. Sham and stroke mice were then housed together in their home cages (group housing) to minimize the detrimental effects of social isolation [21]. Mice used for stroke (or sham) underwent pre-screening with the Barnes maze and open field test. All mice escaped to the dark box in the Barnes maze within three minutes and were thus included in the study.

Three mice died in the vehicle MCAO group (days 4 (2 mice) and 7 (1 mouse) post-MCAO), and three mice in sgp130MCAO (days 4 (2 mice) and 7 (1 mouse)). These mice were excluded from the day 7 analysis but were included in the pre-MCAO analysis. We observed no mortality in the 24-hour male and female cohorts. No mortality was observed in 7-day male cohorts. Vehicle or sgp130 (0.5 mg/kg or 1 mg/kg (females only), i.p., R&D systems; #: 468-MG) was administered immediately after reperfusion in both males and females. A total of four injections were administered, with the first dose given at the time of reperfusion and the remaining injections administered at three-day intervals. BrdU (Sigma, 50 mg/kg, i.p.) was administered for 10 days starting on day one post-MCAO.

Behavioral testing

Neurological deficit scoring was done on day one post-MCAO and the mice were euthanized after the testing. Open field and Barnes maze tests were performed on day 7 and day 28 post-MCAO in the chronic cohort. The animals were euthanized on day 30 post-MCAO. Behavioral studies were conducted and analyzed by a trained observer blinded to surgical and treatment groups. Each testing apparatus was cleaned with 70% ethanol between mice.

Neurological deficit scores

The NDS was assessed on day 1 post-MCAO to quantify acute neurological deficits [22]. The NDS system was defined as follows: 0, no deficit; 1, forelimb weakness and torso turning to the ipsilateral side when held by the tail; 2, circling to the affected side; 3, unable to bear weight on the affected side; and 4, no spontaneous locomotor activity or barrel rolling.

Open field testing

Locomotor activity was assessed as described previously on days 7 and 28 after MCAO [23]. Mice were placed in a brightly lit box, 50 cm wide × 50 cm long × 38 cm high, and allowed to explore freely for 5 min. The mice were filmed from above during the test. These videos were then analyzed using Noldus EthoVision behavioral software (Leesburg, VA).

Barnes maze task

The Barnes maze was performed on the elevated circular platform (9 cm in diameter) with 20 equally spaced holes (5 cm in diameter). A randomly chosen hole was designated as the escape hole that allowed the mouse to escape the platform in a dark box below. Training phase (Pre-surgery training phase): the mouse was placed at the center of the maze and allowed to explore for 5 min. Visual cues on the surrounding walls helped orient the mouse to the position of the escape box. At the end of 5 min, the mouse was gently moved to the dark box and remained there for 1 min. On days 2–4, the mouse was allowed to explore the maze for 3 min, and the time to escape and the number of incorrect entries were recorded. If the mouse failed to find the dark box within 3 min, it was gently guided to the box. Mice received the training twice a day followed by testing on day 5. On day 5, baseline testing was conducted. The mice performed the task twice and the average was taken. On days 2–5 (training and baseline), as well as days 7 and 28 (testing). Peanut butter was used as an olfactory cue, and placed in the dark box to motivate the mice to locate it. Only mice that located the dark box within 3 min were included in the study. All the mice that performed the task were able to locate the dark box within 3 min. The mice were then tested on days 7 and 28 post-MCAO to assess long-term memory retention.

Nest building test

The nest building test was performed and analyzed as described previously [24, 25]. Mice were singly housed overnight in a cage with corncob bedding and one square nestlet (2×2 inches). Twelve hours later photographs were taken of the nests and scored using a 5-point scale. (1) The Nestlet is untouched, with more than 90% intact. (2) The Nestlet is partially torn, but more than 50% remains intact. (3) The Nestlet is almost or completely torn, with no identifiable nest site present (pieces scattered throughout the cage). (4) The Nestlet is almost or completely torn, with an identifiable nest site, but more than 50% of the nest's sides are flat. (5) The Nestlet is almost or completely torn, with an identifiable nest site, and the nest's walls are higher than the body of the mouse on all sides.

Tissue harvesting procedure

Mice were euthanized on day 3 (acute cohort) and day 30 (chronic/recovery cohort) post-MCAO. Mice were euthanized on day 3 (acute cohort) and day 30 (chronic/recovery cohort) post-MCAO. Animals were transcardially perfused with 40 ml of cold sterile PBS. The olfactory bulb, brainstem, and cerebellum were removed.

2,3,5-Triphenyltetrazolium chloride (TTC) staining

Brains were placed at -80°C for 4 min to slightly harden the tissue. Five 2-mm coronal sections were then cut from the frontal pole to the cerebellar junction and stained with 1.5% TTC (SIGMA, St. Louis, MO). Slices were fixed in 4% formalin and then digitized for assessing infarct volume using Fiji software (version 2.9.0). Infarct volume (mm^3) = (Infarct volume) - (Contralateral / Ipsilateral volume).

Cresyl violet (CV) staining procedure

CV staining was performed as described previously. The brain was post-fixed overnight in 4% paraformaldehyde [26] and placed in a 30% sucrose solution for 48 h before processing. The brains were then cut into 30- μm sections on a freezing microtome, and every eighth slice was stained with CV to visualize tissue loss. The slices were digitally imaged, and tissue atrophy was analyzed using Fiji software. Tissue atrophy percentage was calculated using the following formula: percentage tissue atrophy = (total ipsilateral tissue / total contralateral tissue) \times 100.

Flow cytometry procedure

Brain tissue was harvested at 72 h or 7 days post-MCAO, placed in RPMI medium (Lonza), and processed by mechanical and enzymatic digestion using collagenase/dispase (1 mg/mL) and DNase (10 mg/mL; Roche Diagnostics) as previously described [27]. The cell suspension was filtered through a 70 μm filter, and leukocytes were isolated from the interphase of a 70%/30% Percoll gradient. Spleens were mechanically disrupted through a 70 μm filter screen, and blood was collected in heparinized tubes. Red blood cell lysis was achieved with two consecutive 5–10 min incubations in Tris-ammonium chloride (Stem Cell Technologies). Leukocytes were washed with 1X PBS and blocked with mouse Fc Block (eBioscience, 1 μl /50 μl) before staining with primary antibody-conjugated fluorophores: CD45-R718, CD11b-BV605, F4/80-PE/Cy7, Ly6C-APC, Ly6G-ef450, CD3-APC-ef780, IL-6R-APC or PE, and gp130-PE. For intracellular IL-6 and phosphorylated STAT3 (pSTAT3) staining, cells were fixed and permeabilized using a fixation/permeabilization kit (BD Biosciences) according to the manufacturer's instructions. Cells were incubated with IL-6-APC or pSTAT3-Percp Cy5.5-conjugated antibodies overnight at 4°C , followed by washing. Data

acquisition was performed on a CytoFLEX cytometer (Beckman Coulter) and analyzed using FlowJo software (TreeStar Inc.). Cell-specific fluorescence minus one control was used to validate antibody specificity. For leukocyte IL-6R and gp130 estimation in the brain, no fewer than 200,000 events were recorded. For blood IL-6, IL-6R, and gp130 estimation, no fewer than 100,000 events were recorded.

Immunohistochemistry (IHC)

IHC staining was performed on 30- μm mouse brain sections mounted on Fischer Scientific Superfrost Plus charged slides as described previously [25]. Tissue sections were briefly rinsed in 0.1 M phosphate-buffered saline (PBS), pH 7.4. Antigen retrieval was performed by heating the tissue in a 10 mM sodium citrate buffer at pH 6.0. Tissue sections were incubated for 1 h in blocking solution (0.1% Triton-X, 10% normal goat serum in 1X PBS), followed by overnight incubation with the primary antibody at 4°C : IBA-1 (Fujifilm Wako Pure Chemical Corporation, #NCNP24, 1:200); GFAP-Cy3 (Sigma-Aldrich, #C9205, 1:300); DyLight 594-labeled Lycopersicon Esculentum (tomato) lectin (Vector Laboratories, 1:300); Doublecortin (Cell Signaling, #14802S, 1:300); BrdU (Abcam, #ab6326, 1:100); IL-6 (Thermo Fisher Scientific, #MA5-45069, 1:100). To quantify neurogenesis, sections were washed three times with 0.1 M PBS (pH 7.4) for 10 min, then placed in ice-cold 1 N hydrochloric acid (HCl) for 10 min, followed by incubation in 2 N HCl for 30 min at 37°C . After 30 min, sections were rinsed three times with 0.1 M 1X PBS and incubated in 0.1 M boric acid for 10 min. Sections were washed three times, blocked with blocking solution, and incubated overnight with BrdU antibody at 4°C . Digital images were taken on a Leica microscope. Three coronal brain sections per mouse, taken 0.02, 0.45, and 0.98 mm from bregma, were stained and visualized for quantification at 20X magnification at the core/penumbra junction to quantify positive cells. Three images were taken from each mouse brain, and values were averaged.

Enzyme-linked immunosorbent assay (ELISA)

The IL-6 (MBS705090), IL-6R (MBS041720), and LBP (KA0449) ELISAs were performed according to the manufacturer's instructions. For the IL-6 assay, undiluted plasma was used. Plasma samples were diluted 1:20 in dilution buffer for the IL-6R assay and 1:800 for the LBP assay.

Statistical analysis

Data are presented as mean \pm SEM, except for NDS, which is presented as median (interquartile range) and analyzed using the Mann-Whitney test. Outliers were identified using the ROUT test. Two-group comparisons

were analyzed using an unpaired t-test with Welch's correction. Flow cytometry data were analyzed using two-way ANOVA with Tukey's multiple comparisons test. Data from three groups were analyzed using ordinary one-way ANOVA with Tukey's multiple comparisons test. Statistical significance was set at $p < 0.05$.

Results

Induction of MCAO in young male mice leads to an increase in expression of IL-6, but a decrease in membrane IL-6R acutely after stroke

IL-6 signals by binding to mIL-6R followed by gp130 to initiate signaling. We investigated the expression of IL-6, mIL-6R, and mgp130 acutely (72 h) in the blood after MCAO using flow cytometry (Suppl. Figure 1). The induction of MCAO led to a significant increase ($p < 0.05$) in the mean fluorescence intensity (MFI) of IL-6 on live cells compared to sham-operated controls. MCAO also

resulted in a decrease in mIL-6R expression on live cells; however, there was no difference observed between MCAO and sham-operated mice in the MFI of mgp130. These findings indicate that stroke increases IL-6 expression and decreases mIL-6R expression, with no changes in mgp130 expression.

Inhibition of IL-6 trans-signaling improves NDS and reduces infarct volume 24 h after stroke in young male mice

We investigated the efficacy of sgp130 on infarct volume 24 h post-stroke, as the lesion is fully developed within this timeframe [28]. Given the exploratory nature of this research, we administered sgp130 at a dosage of 0.5 mg/kg at the time of reperfusion (Fig. 1A). This dosage was chosen based on literature demonstrating its efficacy in reducing atrial fibrillation, improving disease severity in experimental ulcerative colitis models, and regressing

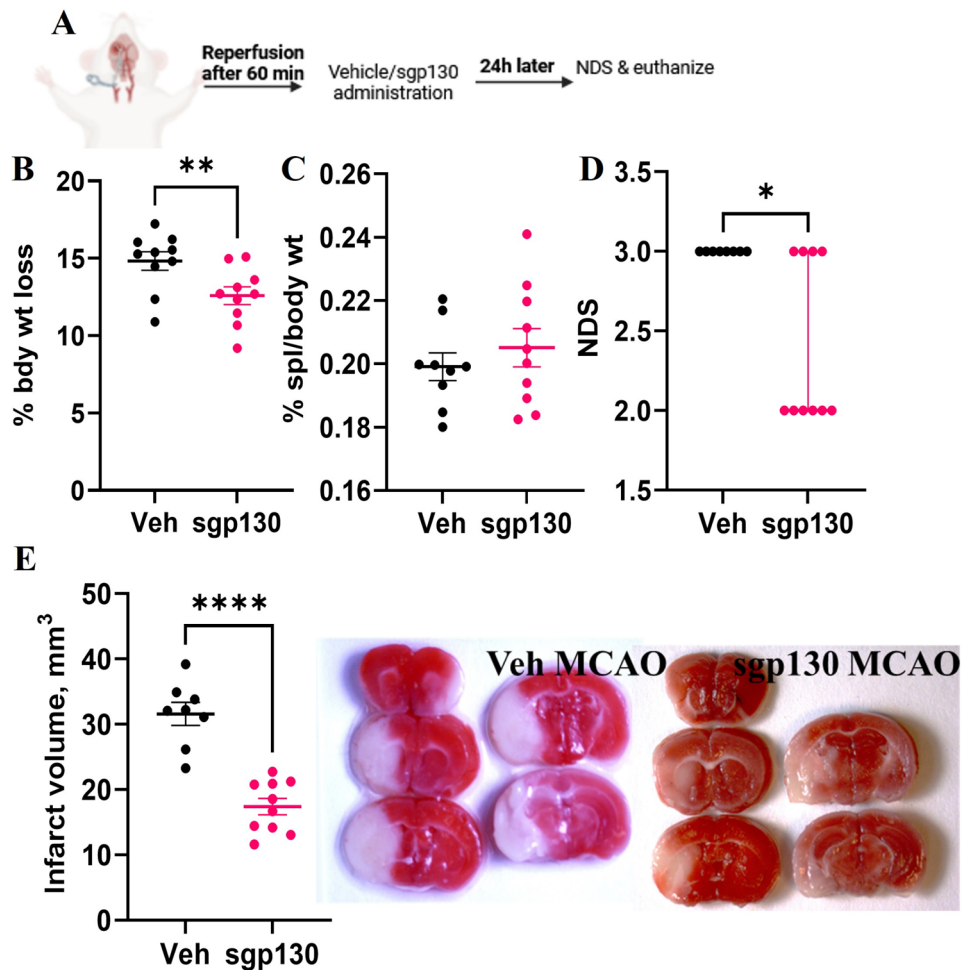


Fig. 1 Inhibition of IL-6 trans-signaling improves NDS and reduces infarct volume 24 h after stroke in young male mice. **(A)** Experimental strategy for 24 h studies. **(B)** percentage body weight loss. **(C)** percentage spleen body weight. **(D)** Neurological deficit scores (NDS). **(E)** Infarct volume quantification and representative image of infarct in the vehicle and sgp130 treated groups. Data presented as mean \pm SEM. $n = 8-10$ /gp. Data were analyzed using the Unpaired t-test with Welch's correction. NDS analyzed by Mann Whitney test and presented as a Median with an interquartile range. * $p < 0.05$; ** $p < 0.01$, **** $p < 0.001$

atherosclerosis in hypercholesterolemic mice [13, 29, 30]. Mice treated with sgp130 exhibited a significantly lower percentage of body weight loss ($p < 0.05$) compared to vehicle-treated MCAO mice at 24 h post-MCAO (Fig. 1B), vehicle-treated mice lost more weight after experimental stroke. Acute splenic atrophy is a common occurrence in experimental stroke models and contributes to brain injury. Interestingly, we found no significant difference in spleen/body weight% between sgp130-treated and vehicle-treated MCAO mice at 24 h (Fig. 1C). The Neurological Deficit Score (NDS) was notably lower ($p < 0.05$, Fig. 1D) in animals treated with sgp130 compared to vehicle-treated male mice. Additionally, sgp130 treatment resulted in reduced infarct volume ($p < 0.05$, Fig. 1E) compared to vehicle-treated mice, indicating that inhibition of IL-6 trans-signaling at the time of reperfusion provides neuroprotective effects.

Sgp130 treatment improves post-stroke cognitive decline at sub-acute and chronic time points in young male animals

Following the acute studies, we investigated the inhibition of IL-6 trans-signaling on functional outcomes at subacute (week 1) and chronic time points after stroke (week 2; Fig. 2A). On day 7 post-MCAO, latency to escape and the number of incorrect entries were increased ($p < 0.05$) in vehicle-treated MCAO mice compared to sham-operated mice (Fig. 2B) reflecting stroke-induced cognitive impairment. However, no difference in escape latency or incorrect entries was observed between sham and sgp130-treated MCAO mice at this time point. Vehicle-treated mice took longer to escape and made more incorrect entries than sgp130 MCAO mice. In the open-field test, vehicle-treated mice moved a greater distance than sham-operated mice, reflecting persistent habitual impairment [31, 32]. However, no difference in distance moved was observed between sham and sgp130-treated animals at day 7 post-MCAO. Similarly, vehicle-treated and sgp130-treated MCAO mice traveled similar distances in the open field.

On day 28 post-MCAO, stroke-induced cognitive deficits persisted when comparing sham versus vehicle-treated MCAO animals (Fig. 2C). Latency to escape on the Barnes maze was significantly higher ($p < 0.05$) in the vehicle-treated MCAO mice compared to sham-operated. No difference in latency to escape and number of incorrect entries was observed between sgp130 MCAO mice versus sham-operated animals. Sgp130-treated MCAO mice were able to locate the hidden platform more quickly and with fewer incorrect entries ($p < 0.05$) compared to vehicle-treated MCAO animals. On open field, vehicle-treated MCAO mice traveled longer distances than sgp130 MCAO-treated animals. The vehicle-treated MCAO mice had lower nest-building scores

than the shams reflecting memory impairment. Sgp130-treated MCAO mice demonstrated higher nest-building scores than vehicle-treated mice. These results indicate that treatment with sgp130 resulted in improvements in cognitive functions at subacute and chronic time points, suggesting a beneficial role of inhibiting IL-6 trans-signaling by sgp130 in the functional recovery from stroke.

Sgp130 treatment resulted in reduced tissue loss, inflammation, and SVZ IL6 in young male mice

Sgp130-treated MCAO mice had significantly ($p < 0.05$) reduced tissue loss compared to vehicle-treated MCAO animals after stroke (Fig. 3A). The stroke resulted in increased ($p < 0.05$) markers of inflammation in the peri-infarct regions, including Iba-1 and GFAP⁺ cells in the peri-infarct area compared to the sham (Fig. 3B). Iba-1 and GFAP⁺ cells were significantly lower ($p < 0.05$) in the sgp130-treated MCAO mice compared to the vehicle-treated MCAO group (Fig. 3B). Angiogenesis and neurogenesis are integral to post-stroke recovery [33]. We used *Lycopersicon esculentum* (tomato) lectin, DyLight 649, to stain vessels. The percentage lectin⁺ area in the peri-infarct region was significantly increased ($p < 0.05$) in both vehicle-treated and sgp130-treated MCAO compared to sham-operated (Suppl. Figure 2). However, the sgp130 treatment did not result in an additional change in the percentage of lectin⁺ area compared to vehicle-treated MCAO mice. To determine the contribution of neurogenesis to post-stroke recovery, we examined DCX, a marker for immature neurons, and BrdU in the sub-ventricular zone (Fig. 3C). A significant increase ($p < 0.05$) in SVZ DCX⁺ cells was observed in both vehicle-treated and sgp130-treated MCAO mice compared to sham-operated mice. The sgp130-treated MCAO group had a significantly higher ($p < 0.05$) number of SVZ DCX⁺ cells compared to vehicle-treated animals. Furthermore, an increase in SVZ BrdU⁺ cells was evident in both vehicle and sgp130-treated MCAO mice compared to sham. Although not significant ($p = 0.064$), sgp130-treated MCAO mice had a higher number of BrdU⁺ cells compared to vehicle-treated MCAO animals. Brain IL-6 facilitates neurogenesis [34, 35], we observed higher SVZ IL-6 intensity in MCAO groups compared to sham-operated animals (Fig. 3D). Sgp130-treated MCAO mice had significantly higher SVZ IL-6 intensity compared to vehicle-treated MCAO animals. These findings suggest that inhibiting peripheral IL-6 signaling post-stroke promotes tissue recovery by reducing neuroinflammation. Furthermore, the observed increase in central IL-6 signaling in sgp130-treated mice may facilitate neurogenesis, thereby supporting cognitive recovery.

IL-6 promotes anti-inflammatory signaling via mIL-6R. Studies indicate that immune cells and hepatocytes are major sources of sIL-6R in circulation during acute

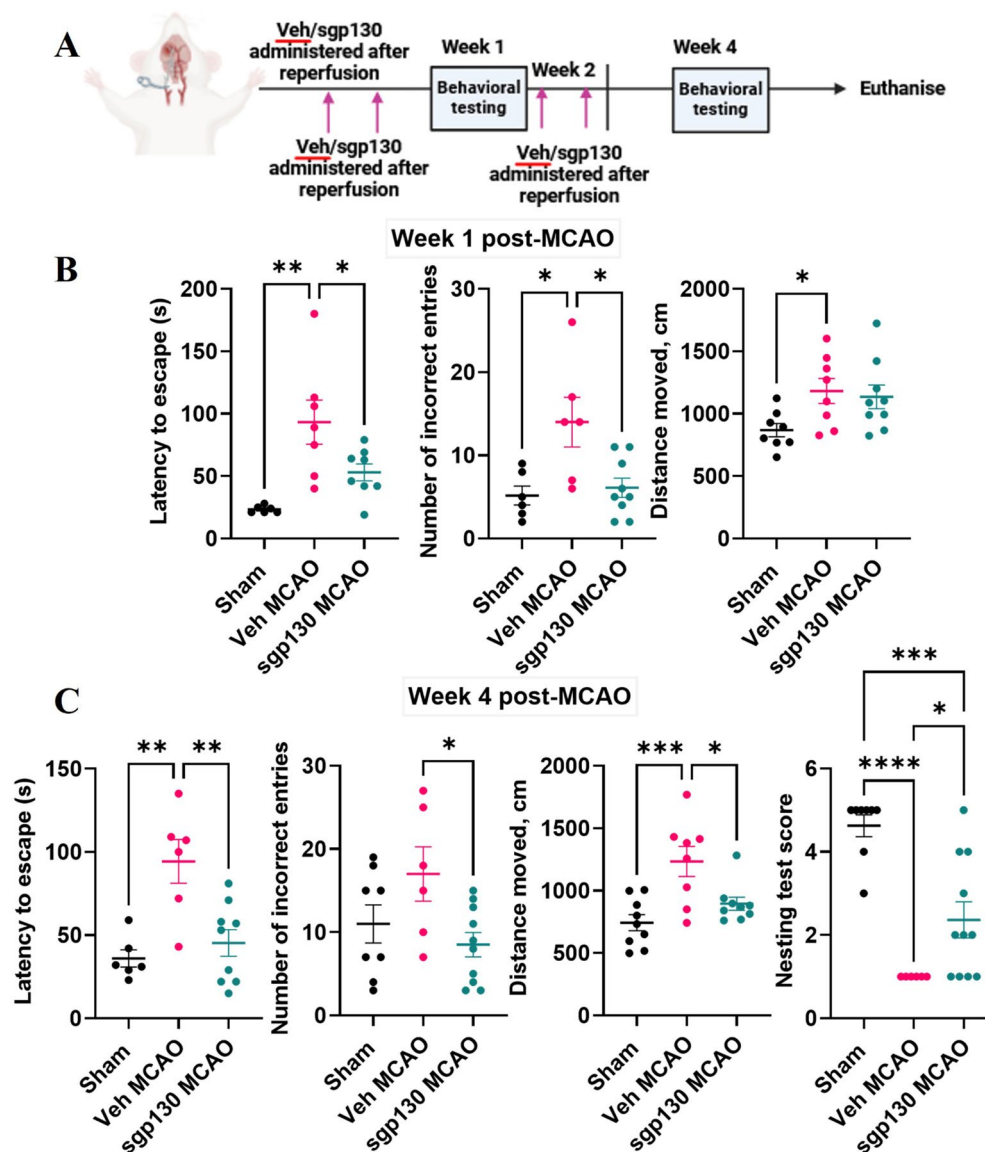


Fig. 2 Sgp130 treatment improves post-stroke cognitive decline at sub-acute and chronic time points in young male animals. **(A)** Experimental strategy for 30 days studies. **(B)** latency to escape, number of incorrect entries on Barnes maze, and distance moved on an open field at week 1 post-MCAO. **(C)** latency to escape, number of incorrect entries on Barnes maze, and distance moved on an open field and nest building assessment at week 4 post-MCAO. Data presented as mean \pm SEM. $n=6-10$ /gp. Three group data were analyzed by Ordinary one-way ANOVA with Tukey's multiple comparisons test. * $p < 0.05$, ** $p < 0.01$, *** $p < 0.001$

phase responses [36, 37], with sIL-6R being generated by proteolytic cleavage in mice. Given these findings, we hypothesized that increased mIL-6R expression on immune cells might correlate with reduced cleavage of this receptor. To test this hypothesis, we investigated the expression of mIL-6R and membrane gp130 (mgp130) at day 7 post-MCAO, a critical recovery time associated with the initiation of cognitive recovery. The mean fluorescence intensity (MFI) of mIL-6R on live brain cells was significantly higher in mice treated with sgp130 after stroke. However, no difference in mgp130 MFI on brain live cells was observed between vehicle-treated MCAO

and sgp130-treated MCAO mice (Fig. 3E). Although, non-significant, splenic live cells in the sgp130-treated had higher MFI mIL-6R than the vehicle-treated MCAO mice. There was no difference in the mgp130 MFI on splenocytes between sgp130-treated and vehicle-treated MCAO mice, indicating that central IL-6/mIL-6R signaling remained intact in sgp130-treated MCAO mice. These results suggest that while peripheral IL-6 signaling was partly inhibited after stroke, central IL-6/mIL-6R signaling remained unaffected in the sgp130-treated mice. This preservation of central IL-6/mIL-6R signaling in

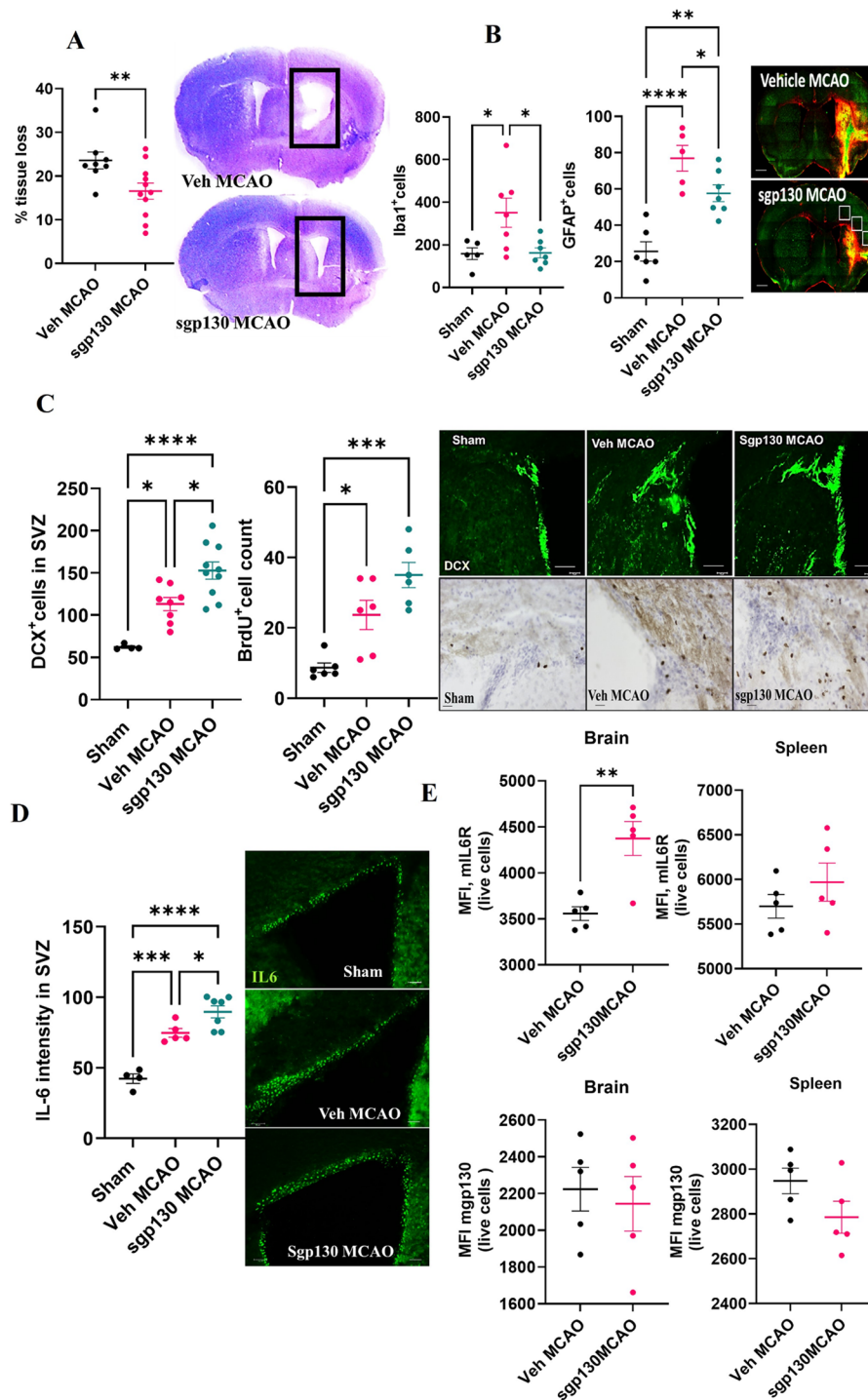


Fig. 3 Sgp130 treatment resulted in reduced tissue loss, inflammation, and SVZ IL6 in young male mice. **(A)** on percentage tissue loss. **(B)** Iba1 [62] and GFAP (red) positive counts in peri-infarct region. **(C)** Doublecortin [62] and BrdU positive cells in SVZ. **(D)** IL-6 intensity in the SVZ. **(E)** Membrane IL-6R [62] and gp130 MFI on live brain cells and splenocytes at day 7 post-MCAO by flow cytometry. Data presented as mean \pm SEM. $n=6-10$ /gp. Two group comparisons were analyzed by Unpaired t-test with Welch's correction and three group data were analyzed by Ordinary one-way ANOVA with Tukey's multiple comparisons test. * $p < 0.05$, ** $p < 0.01$, *** $p < 0.001$

sgp130-treated mice could contribute to improved outcomes in cognitive recovery post-stroke.

Sgp130 treatment did not improve cognitive functions, tissue loss, and neuroinflammation after stroke in young female mice

Inhibition of IL-6 signaling resulted in improved cognitive outcomes in young male animals; hence, we tested the efficacy of sgp130 in young females after stroke (Suppl. Figure 3). There was no difference in the neurological deficit score (NDS) between vehicle-treated and sgp130-treated MCAO females at day 7 post-stroke (Suppl. Figure 3B). Furthermore, no difference in the distance moved in the open field test was observed between the two MCAO groups. The latency to escape was not different; however, sgp130 MCAO-treated females made significantly ($p < 0.05$) fewer incorrect entries compared to vehicle-treated female mice (Suppl. Figure 3B). On day 14 post-stroke, sgp130-treated females moved a significantly greater distance ($p < 0.05$) compared to vehicle-treated MCAO mice in the open field test (Suppl. Figure 3C). However, no differences between the two MCAO groups were evident in latency to escape or the number of incorrect entries in the Barnes maze. Similarly, no differences in nest-building scores were observed between sgp130-treated and vehicle-treated MCAO female animals (Suppl. Figure 3C). Furthermore, the histopathological analysis revealed no difference in the percentage of tissue loss (Suppl. Figure 3D), Iba1, and GFAP⁺ cells (Suppl. Figure 3D) in the peri-infarct area between the two-stroke groups, indicating similar levels of neuroinflammation and tissue damage. Together, these findings suggest that prolonged inhibition of IL-6 signaling using sgp130 does not improve functional outcomes,

tissue recovery, or neuroinflammation in young female mice after stroke.

Higher levels of systemic IL-6 and sIL-6R levels 24 h after stroke in mice

To explore the potential reasons behind the lack of efficacy of sgp130 in females, we measured plasma levels of IL-6 and sIL-6R in mice following stroke (Fig. 4). Stroke induction led to a significant increase in systemic IL-6 levels (Fig. 4A). In male mice (Fig. 4B), IL-6 levels were 18.80 ± 3.30 pg/ml in the sham group compared to 30.92 ± 3.22 pg/ml after MCAO ($p < 0.05$). Similarly, in female mice (Fig. 4C), IL-6 levels were 10.16 ± 1.94 pg/ml in the sham group compared to 31.48 ± 5.24 pg/ml after MCAO ($p < 0.01$). These results suggest that female mice experienced a more pronounced increase in plasma IL-6 levels following stroke. Additionally, female mice exhibited higher levels of circulating sIL-6R following MCAO compared to sham-operated females. In contrast, no difference in IL-6R levels was observed between male MCAO and sham mice (Fig. 4D). Notably, female MCAO mice had significantly higher sIL-6R levels than their male counterparts. These findings suggest that a higher dose of sgp130 might be necessary to effectively inhibit IL-6 trans-signaling in female mice.

IL-6 expression on monocytes and neutrophils is higher in female mice 24 h after stroke

The percentage of IL-6-positive cells increased in both male and female mice after stroke compared to their respective sham-operated groups (Suppl. Figure 4). In males, this increase was observed in both Ly6C⁺ monocytes and Ly6G⁺ neutrophils (Suppl. Figure 4B), with significantly higher percentages of IL-6-positive cells in these populations post-stroke compared to

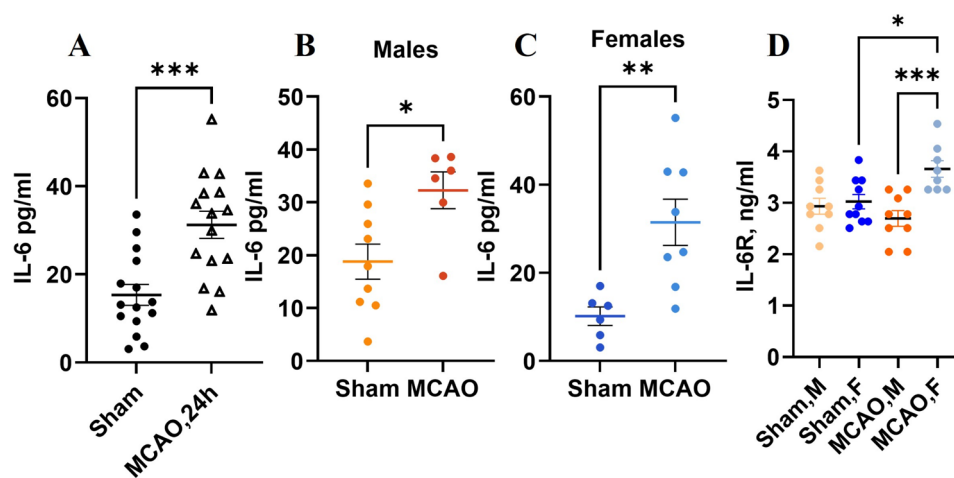


Fig. 4 Systemic IL-6 and IL-6R levels increased at 24 h in mice after stroke. **(A)** Plasma IL-6 levels in mice sham and 24 h after MCAO. **(B)** Plasma levels in males. **(C)** Females. **(D)** sIL-6R levels. Data presented as mean \pm SEM. $n = 6-9$ /gp. Two group comparisons were analyzed by Unpaired t-test with Welch's correction and by Ordinary one-way ANOVA with Tukey's multiple comparisons test. * $p < 0.05$; ** $p < 0.01$

sham-operated males. However, no significant increase in the percentage of IL-6-positive Ly6C⁺ monocytes and Ly6G⁺ neutrophils was observed in female mice after stroke compared to female sham groups. Notably, the percentage of IL-6-positive monocytes and neutrophils was significantly lower in female mice compared to males after stroke (Suppl. Figure 4B).

An increase in the mean fluorescence intensity (MFI) of IL-6 in live cells was observed in both male and female mice after MCAO compared to their respective sham groups (Suppl. Figure 4 C). Notably, a significant increase ($p < 0.05$) in IL-6 MFI on live cells was observed in females compared to males following stroke. MCAO led to a rise in IL-6 MFI in monocytes and neutrophils in both male and female mice (Suppl. Figure 4 C). However, this increase in IL-6 MFI was significantly higher in female mice compared to male mice after stroke. These findings suggest that, despite a lower percentage of IL-6-positive cells in females, they exhibit higher levels of IL-6 expression after stroke.

Inhibition of IL-6 trans-signaling does not elevate systemic LBP or IL-6 levels in both males and females after stroke

Post-stroke infections are a major cause of mortality, so we investigated systemic levels of

lipopolysaccharide-binding protein (LBP), a potential marker of sepsis [38]. We observed no significant difference in plasma LBP levels between sham-operated and MCAO male mice (Suppl. Figure 5 A). Similarly, there was no variance in plasma LBP levels between vehicle-treated and sgp130-treated MCAO male animals at day 30 post-stroke. Additionally, systemic levels of IL-6 showed no difference between sham-operated and stroke groups in males, and there was no disparity in plasma IL-6 levels between vehicle-treated and sgp130-treated MCAO groups at day 30 post-stroke.

In female mice, plasma LBP levels were comparable between vehicle-treated and sgp130-treated MCAO groups at day 14 post-stroke (Suppl. Figure 5B). However, although not statistically significant ($p = 0.058$), the sgp130-treated group showed higher plasma IL-6 levels compared to vehicle-treated animals at day 14 post-stroke. These findings suggest that systemic LBP levels remain unaffected by sgp130 treatment in both males and females at days 30 and 14 post-stroke, respectively.

A higher dose of sgp130 improves neurological deficit score and reduces infarct volume after acute stroke

To test our hypothesis that a higher dose of sgp130 could improve acute stroke outcomes in female mice, we administered 1 mg/kg of sgp130 to young females. We also administered sgp130 at the standard dose of 0.5 mg/kg (same as used for males) at the time of reperfusion (Fig. 5). Twenty-four hours after MCAO, we found no difference in the percentage of body weight loss (Fig. 5A) or in the percentage of spleen to body weight (Fig. 5B) between the vehicle-treated group and those treated with either dose of sgp130 (0.5 mg/kg or 1 mg/kg). However, the group treated with 1 mg/kg of sgp130 showed a significant reduction in the NDS compared to the vehicle-treated MCAO group (Fig. 5C). Additionally, the higher dose of sgp130 significantly reduced the infarct volume compared to the vehicle-treated MCAO group (Fig. 5D), indicating that indeed the higher dose of sgp130 was effective in improving stroke outcomes in female mice.

A higher dose of sgp130 improved long-term functional outcomes in females

Inhibition of IL-6 trans-signaling with a 1 mg/kg dose of sgp130 resulted in reduced distance traveled by females compared to vehicle-treated MCAO females at week 1 post-MCAO (Fig. 6A). While no difference in latency to escape was observed between vehicle-treated and sgp130-treated MCAO females, those treated with 1 mg/kg sgp130 exhibited a reduction in the number of incorrect entries (Fig. 6A). At week 4 post-MCAO, sgp130-treated females demonstrated shorter distances moved in the open field test compared to vehicle-treated mice, indicating persistent habitual impairment (Fig. 6B).

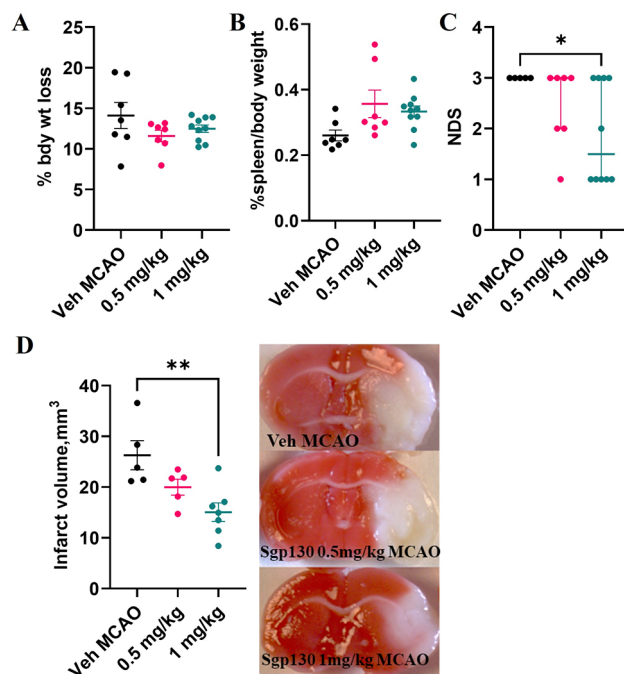


Fig. 5 Sgp130 at higher dose, improved neurological deficit score, and reduced infarct volume in young females at 24 h after stroke. **(A)** Percentage of body weight loss. **(B)** Percentage of spleen/body weight. **(C)** NDS. **(D)** Infarct volume. Data presented as mean ± SEM. $n = 5-10$ /gp. NDS was analyzed by Kruskal-Wallis with Dunn's multiple comparison test and presented as a Median with an interquartile range. * $p < 0.05$; ** $p < 0.01$, *** $p < 0.001$

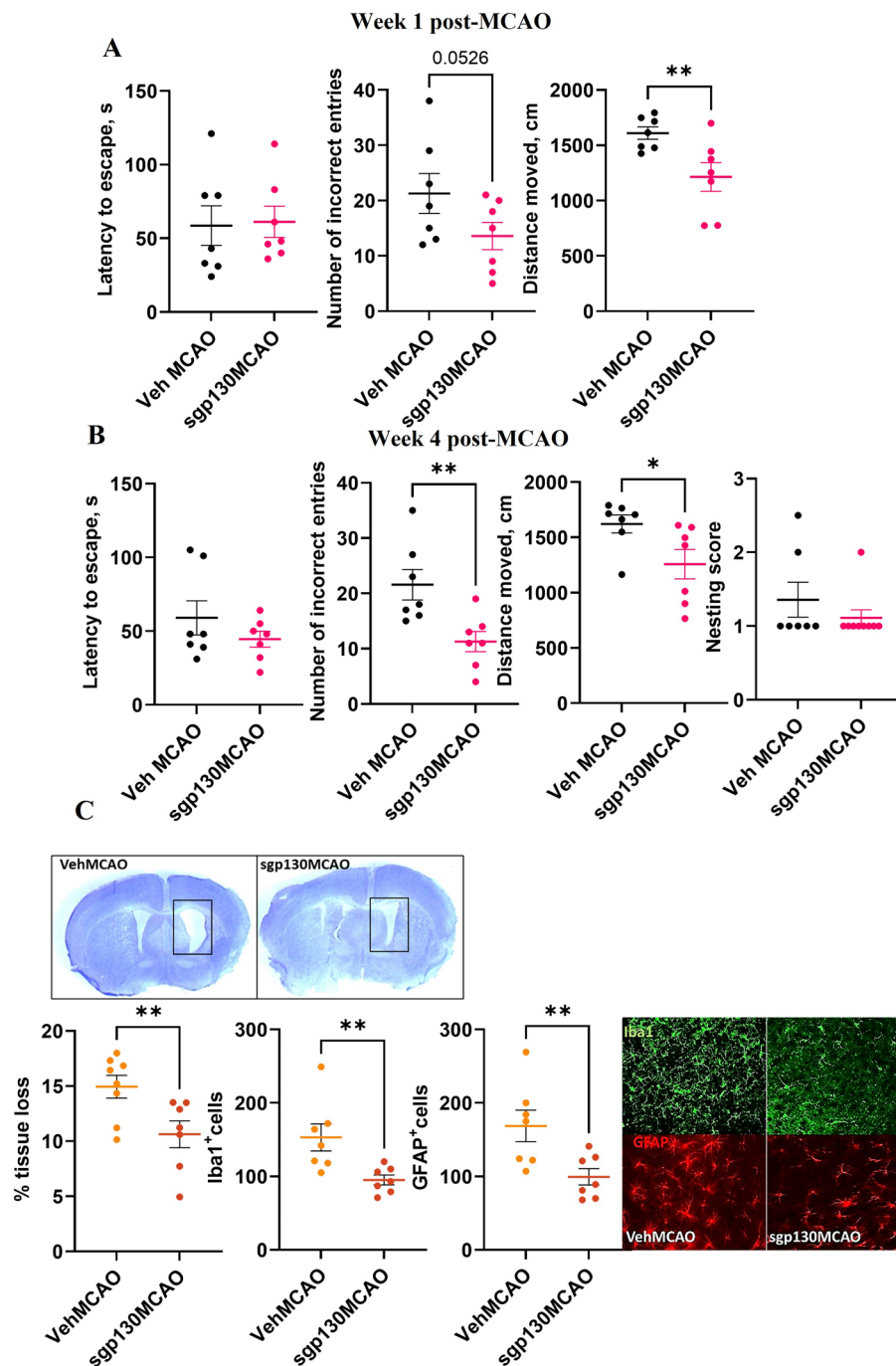


Fig. 6 Treatment with sgp130 resulted in improvement in post-stroke cognitive function and reduced tissue loss and inflammation in the young female mice. **(A)** latency to escape, number of incorrect entries on Barnes maze, and distance moved on an open field at week 1 post-MCAO. **(B)** latency to escape, number of incorrect entries on Barnes maze, and distance moved on an open field and nest building assessment at week 4 post-MCAO. **(C)** on percentage tissue loss, Iba1 [62] and GFAP (red) positive counts in peri-infarct region. Data presented as mean \pm SEM. $n=7/gp$. Two group comparisons were analyzed by Unpaired t-test with Welch's correction. * $p < 0.05$, ** $p < 0.01$

However, sgp130-treated females continued to make fewer incorrect entries, with no differences in latency to escape. Additionally, nesting scores between the two groups remained unchanged at week 4. Females treated with sgp130 had significantly reduced percentage tissue

loss than vehicle-treated mice (Fig. 6D). Furthermore, a decline in Iba1 and GFAP⁺ cells was observed in sgp130-treated MCAO females compared to vehicle-treated mice (Fig. 6D), suggesting that at higher dose sgp130 effectively mitigated functional and histological deficits.

Targeting IL-6 trans-signaling by sgp130 maintains splenic immune cell mIL-6R and reduces phosphorylation of STAT3 in brain macrophages

To investigate the mechanism responsible for sgp130 efficacy after MCAO, we investigated the expression of IL-6R on splenic macrophages, monocytes, neutrophils, and T cells at day 7 post-MCAO in both male (Fig. 7) and female mice (Fig. 8). In males, although not statistically significant, a decrease in MFI mIL-6R on macrophages

was observed in vehicle-treated MCAO mice compared to sham male mice (Fig. 7A). Notably, a significantly higher ($p < 0.05$) MFI mIL-6R on macrophages was found in sgp130-treated MCAO mice compared to vehicle-treated MCAO mice. A reduced MFI mIL-6R on Ly6C^{hi} monocytes was also observed in vehicle-treated MCAO mice compared to sham male mice (Fig. 7B). Sgp130 treatment resulted in a higher mIL-6R expression on Ly6C^{hi} monocytes than in vehicle-treated MCAO mice

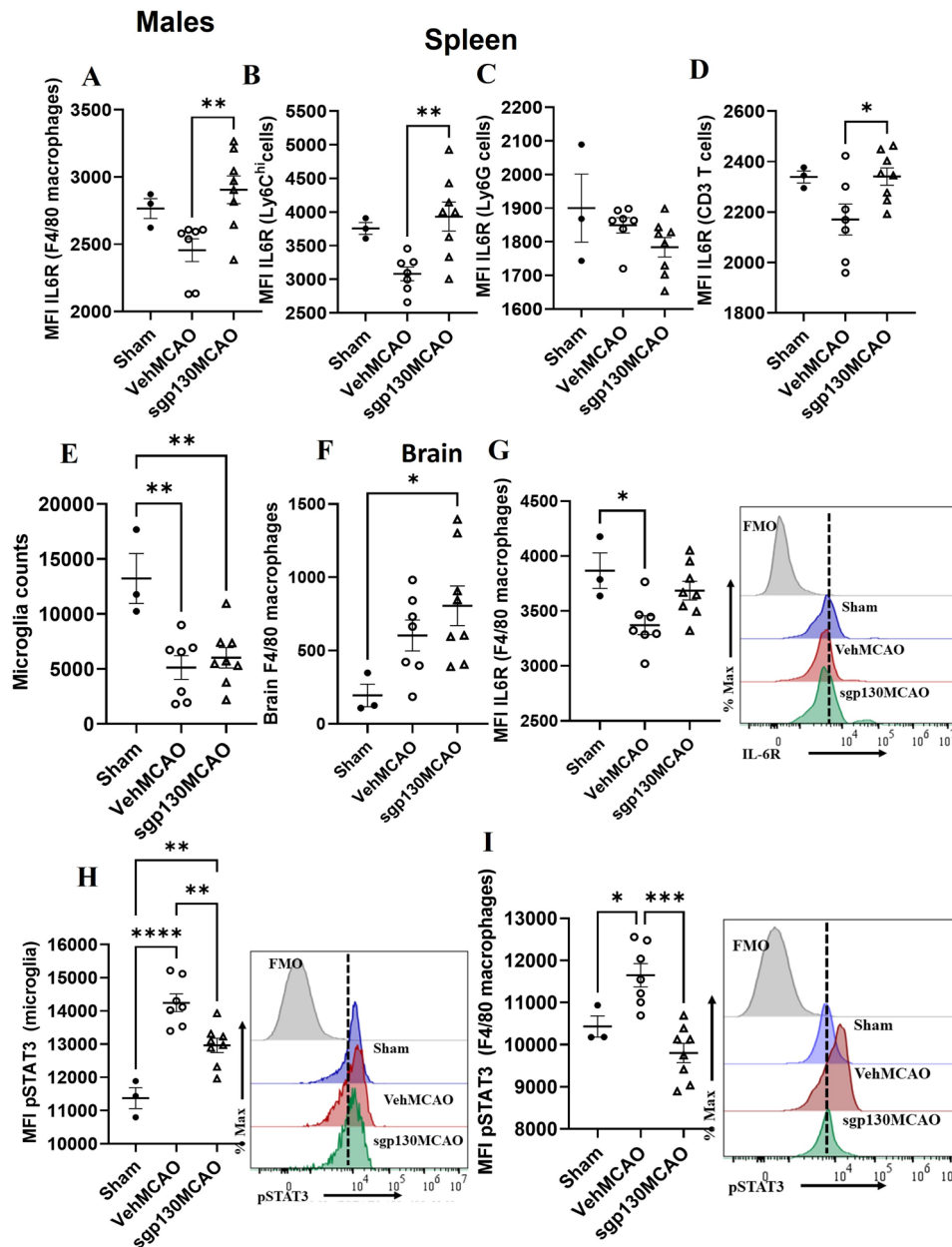


Fig. 7 Sgp130 maintains splenic immune cell mIL-6R reduced brain F4/80 macrophage phosphorylated STAT3 expression at day 7 after MCAO in male animals. Increase in MFI mIL-6R on splenic. **(A)** macrophages, **(B)** Ly6C^{hi} monocytes, **(C)** Ly6G neutrophils and **(D)** CD3 T cells. **(E)** CD45^{int}CD11b⁺ microglia count, **(F)** F4/80 macrophage count, **(G)** MFI mIL-6R on F4/80 macrophages, **(H)** Decrease in MFI pSTAT3 on microglia, **(I)** F4/80 macrophages. Data presented as mean \pm SEM. $n = 3-8$ /gp. Three group data were analyzed by Ordinary one-way ANOVA with Tukey's multiple comparisons test. * $p < 0.05$; ** $p < 0.01$, *** $p < 0.001$

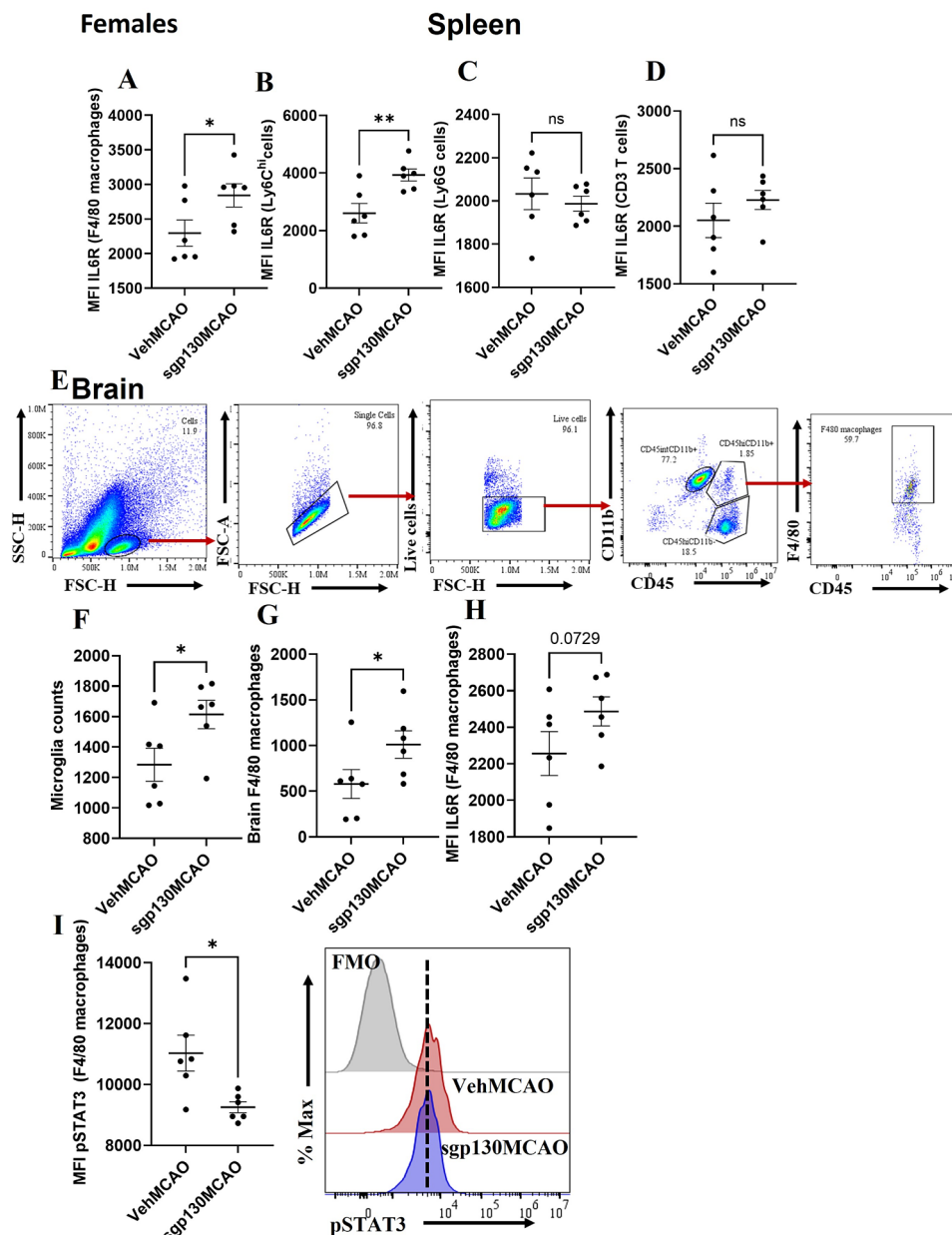


Fig. 8 Sgp130 maintains splenic immune cell mIL-6 reduced brain F4/80 macrophage phosphorylated STAT3 expression at day 7 after MCAO in female animals. Increase in MFI mIL-6R on splenic (A) macrophages, (B) Ly6C^{hi} monocytes, (C) Ly6G neutrophils and (D) CD3 T cells. (E) Representative gating strategy for brain microglia and F4/80 macrophages. (F) CD45^{int}CD11b⁺ microglia count, (G) F4/80 macrophage count, (H) MFI mIL-6R on F4/80 macrophages, (I) Decrease in MFI pSTAT3 on F4/80 macrophages. Data presented as mean \pm SEM. $n = 3-6$ /gp. Two group comparisons were analyzed by Unpaired t-test with Welch's correction. * $p < 0.05$, ** $p < 0.01$

(Fig. 7B). No differences in MFI mIL-6R were observed on neutrophils between sham, vehicle-treated MCAO, and sgp130-treated MCAO mice (Fig. 7C). Additionally, sgp130-treated MCAO mice showed higher MFI mIL-6R on T cells compared to vehicle-treated MCAO mice (Fig. 7D). These findings suggest that sgp130 treatment may help preserve mIL-6R expression and limit the shedding of IL-6R on peripheral macrophages, monocytes,

and T cells following stroke in male mice, thereby reducing IL-6 trans-signaling.

Following MCAO, a decrease in microglia numbers was observed compared to the sham group (Fig. 7E), consistent with previous studies [39]. Although not statistically significant, MCAO led to a higher number of brain F4/80 macrophages than the sham group (Fig. 7F). A significant increase in brain F4/80 macrophages was observed in sgp130-treated MCAO mice compared to the sham

group (Fig. 7F). Additionally, a reduced ($p < 0.05$) expression of mIL-6R was observed on brain F4/80 macrophages in vehicle-treated MCAO mice compared to sham (Fig. 7G). There was no difference in mIL-6R expression on brain F4/80 macrophages between sham and sgp130-treated MCAO mice. Vehicle-treated MCAO mice exhibited an increased MFI of pSTAT3 in microglia and F4/80 macrophages compared to sham (Fig. 7H & I). Sgp130 treatment resulted in a reduced ($p < 0.05$) MFI of pSTAT3 in microglia and F4/80 macrophages compared to vehicle-treated MCAO mice. Previous studies have demonstrated that inhibition of IL-6 trans-signaling by sgp130 reduces pSTAT3 levels in experimental models of SARS-CoV-2 infection, psoriasis, and coronary artery disease [13, 40, 41], and in patients with inflammatory bowel disease [42]. These findings suggest that the beneficial effects of sgp130 treatment in MCAO may be partly mediated by its ability to reduce pSTAT3 expression after stroke.

Similarly, to male mice, female sgp130-treated (1 mg/kg) MCAO mice exhibited higher MFI of mIL-6R on splenic F4/80 macrophages (Fig. 8A) and Ly6C^{hi} monocytes (Fig. 8B) compared to vehicle-treated MCAO mice. No differences in MFI of mIL-6R were observed on splenic neutrophils (Fig. 8C) or T cells (Fig. 8D) between sgp130-treated and vehicle-treated MCAO mice. In the brain, microglia and F4/80 macrophage counts were significantly higher in sgp130-treated MCAO mice compared to vehicle-treated MCAO female mice (Fig. 8F & G, respectively). Although not statistically significant, sgp130-treated MCAO females exhibited a higher MFI of mIL-6R on F4/80 macrophages than vehicle-treated MCAO females but not in microglia (data not shown). Furthermore, sgp130 treatment resulted in a reduced ($p < 0.05$) MFI of pSTAT3 in F4/80 macrophages compared to vehicle-treated MCAO females. These findings suggest that the reduction in pSTAT3 expression on brain F4/80 macrophages could contribute to the beneficial effects of sgp130 treatment in female mice.

Discussion

This study provides novel evidence supporting our hypothesis that inhibiting IL-6 trans-signaling enhances long-term functional outcomes after stroke. We demonstrated that sgp130 treatment significantly improved stroke outcomes in both males and females, though the effects were dose- and sex-dependent. A previous study using a permanent middle cerebral artery occlusion model demonstrated that IL-6 administration alone improved outcomes at 24 h, while co-administration with sIL-6R worsened outcomes [43], suggesting that intensified IL-6 trans-signaling exacerbates injury. Our findings indicate that acute stroke increases IL-6 expression in peripheral blood cells, reflecting systemic inflammation

[14, 44]. Moreover, mIL-6R expression on live peripheral blood cells decreased after stroke, while membrane gp130 expression remained unchanged. The reduction in mIL-6R on blood cells post-stroke may be attributed to the shedding of mIL-6R, which generates sIL-6R [45, 46] and promotes IL-6 trans-signaling [12, 40]. Therefore, we administered sgp130, which selectively inhibits IL-6 trans-signaling without affecting classical signaling pathways [47]. This study is the first to evaluate the efficacy of sgp130 in experimental stroke, with initial administration at reperfusion—a critical event known to exacerbate ischemic damage [48, 49]. Our results revealed that sgp130-treated young males experienced reduced body weight loss, improved neurological deficit scores, and smaller infarcts compared to vehicle-treated controls, highlighting the potential of sgp130 as a therapeutic intervention to mitigate post-stroke damage and enhance recovery, particularly when administered during the acute phase of reperfusion.

Spontaneous functional recovery is typically observed in young animals after stroke [27, 50]. Sgp130 treatment improved acute and long-term outcomes after stroke. At both subacute and chronic time points, sgp130-treated mice demonstrated shorter latency to escape and made fewer incorrect entries in the Barnes maze, indicating improved hippocampal-dependent cognitive recovery [27]. Additionally, sgp130-treated mice traveled a shorter distance in the open field test and exhibited improved nest-building scores, indicating enhanced sensorimotor function and memory [24, 51]. These findings emphasize the beneficial effects of targeting IL-6 trans-signaling in enhancing functional recovery following stroke.

In both preclinical and clinical settings, gliosis is a common occurrence that regulates neuroinflammation following stroke [52, 53]. Treatment with sgp130 reduced the presence of both Iba1⁺ (microglia/macrophage marker) and GFAP⁺ (astrocyte marker) cells in the peri-infarct region, indicating decreased neuroinflammation through inhibition of IL-6 trans-signaling. Neurogenesis and angiogenesis play crucial roles in post-stroke recovery. While we observed no differences in vascular changes, sgp130 treatment enhanced neurogenesis, as evidenced by increased SVZ DCX⁺ and BrdU⁺ cells in sgp130-treated mice. Brain IL-6 trans-signaling promotes neuronal differentiation and neurogenesis in models of traumatic brain injury [54] and stroke [11, 55, 56]. Increased SVZ IL-6 expression in sgp130-treated MCAO mice could partially account for the enhanced SVZ neurogenesis observed in these mice after stroke. While we did not explore brain sIL-6R levels, we found increased brain mIL-6R expression in sgp130-treated MCAO mice, which may be attributed to reduced cleavage of the IL-6R receptor and reduced IL-6 trans-signaling in the brain. These findings suggest that inhibiting IL-6 trans-signaling

with sgp130 not only reduces neuroinflammation but also promotes neurogenesis, potentially contributing to improved recovery following stroke.

Stroke exhibits sexual dimorphism, highlighting the importance of testing therapies in both sexes. At a 0.5 mg/kg dose, sgp130 improved outcomes in males but was ineffective in females. Post-stroke, females exhibited stronger IL-6 induction and higher circulating sIL-6R levels compared to males, suggesting that increased shedding of mIL-6R might reduce the efficacy of this dose, though this hypothesis requires further testing. Furthermore, female monocytes and neutrophils displayed higher IL-6 intensity, indicating fewer cells expressed higher levels of IL-6. Notably, increasing the sgp130 dose to 1 mg/kg improved long-term functional outcomes in females, highlighting dose-dependent efficacy. At this efficacious dose, sgp130 preserved mIL-6R expression on splenic immune cells in both sexes and reduced STAT3 phosphorylation in brain macrophages. A recent study in a cerebrovascular injury mouse model highlights the critical role of IL-6R+ repair-associated Iba1+ cells in functional recovery [57]. Following cerebrovascular injury, the study observed increased IL-6R expression on repair-associated Iba1+ cells in the brain. Infiltrating inflammatory monocytes were identified as the primary source of IL-6, and their absence disrupted the function of these repair-associated cells, leading to impaired cerebrovascular repair and prolonged neurological deficits [57]. By day 7 post-injury, the infiltrating monocytes acquire a microglia-like phenotype [58, 59]. Monocyte-derived macrophages (CD45^{hi}CD11b⁺F4/80⁺) were distinguished from brain-resident microglia (CD45^{int}CD11b⁺). In sgp130-treated mice of both sexes, an increase in brain macrophages with elevated mIL-6R expression and reduced pSTAT3 expression was observed. These changes likely contribute, at least in part, to the long-term functional recovery seen in both males and females.

Given the concerns about IL-6 inhibition and infection risk [60, 61], we assessed systemic LBP and IL-6 levels after stroke. No differences were observed in LBP levels between sgp130-treated and vehicle-treated mice of either sex. Plasma IL-6 levels also remained comparable across groups, suggesting that sgp130 treatment does not exacerbate infection risk.

This study represents the initial investigation into the efficacy of sgp130 in ischemic stroke across both sexes. While this study highlights the therapeutic potential of sgp130, it is limited by the use of young mice, which may not fully represent the clinical population of older stroke patients. Nonetheless, this approach is relevant given the rising incidence of stroke in younger populations [54]. Future research will address the sex-specific effects of IL-6 trans-signaling in older subjects. Additionally,

examining temporal changes in brain and blood IL-6 and sIL-6R levels could identify optimal time points for intervention, enabling more personalized treatment strategies.

In conclusion, this study demonstrates that sgp130 treatment enhances acute and long-term functional outcomes after stroke in a sex- and dose-dependent manner. While 0.5 mg/kg sgp130 was effective in young males, a higher dose (1 mg/kg) was required to achieve similar benefits in young females. By selectively inhibiting IL-6 trans-signaling, sgp130 reduced neuroinflammation, and improved functional recovery, offering a promising therapeutic approach for ischemic stroke.

Abbreviations

IL-6	Interleukin-6
MCAO	Middle cerebral artery occlusion
Gp130	Glycoprotein 130
ELISA	Enzyme-linked immunosorbent assay
IP	Intraperitoneal
mIL-6R	Membrane interleukin-6 receptor
mgp130	Membrane glycoprotein 130
sIL-6	Soluble interleukin-6
ICV	Intracerebroventricular
LPS	Lipopolysaccharides
CBF	Cerebral blood flow
Sgp130	Soluble glycoprotein 130
BrdU	Bromodeoxyuridine or 5-bromo-2'-deoxyuridine
NDS	Neurological deficit scoring
TTC	Triphenyl tetrazolium chloride
CV	Cresyl violet
IHC	Immunohistochemistry
GFAP	Glial fibrillary acidic protein
IBA-1	Ionized calcium-binding adaptor molecule 1
DCX	Doublecortin
pSTAT3	Phosphorylated STAT3
STAT3	Signal Transducer and Activator of Transcription 3

Supplementary Information

The online version contains supplementary material available at <https://doi.org/10.1186/s12974-025-03365-y>.

Supplementary Material 1: Suppl. Figure 1: expression of IL-6, mIL-6R and mgp130 on peripheral blood cells at 72 h after stroke in young male mice by flow cytometry. (A) Representative dot plots showing the gating strategy for live cells. (B) The mean fluorescence intensity (MFI) of the IL-6, mIL-6R and mgp130. (C) Fluorescence minus one (FMO) control are shown in gray while the sham and MCAO groups are color coded. Data presented as mean \pm SEM. $n = 3-6$ /gp. Data were analyzed using the Unpaired t-test with Welch's correction. ****** $p < 0.01$.

Supplementary Material 2: Suppl. Figure 2: Sgp130 treatment did not increase the percentage of lectin-positive (magenta) area in the mice at day 30 post-MCAO. Data presented as mean \pm SEM. $n = 6-10$ /gp. Three group data were analyzed by Ordinary one-way ANOVA with Tukey's multiple comparisons test. ***** $p < 0.05$, ****** $p < 0.01$, ******* $p < 0.001$.

Supplementary Material 3: Suppl. Figure 3: Sgp130 did not treatment ameliorate post-stroke cognitive decline tissue loss or inflammation in young female at 14 days. (A) Experimental strategy for 14 days studies. (B) NDS, distance moved on open field, latency to escape, number of incorrect entries on Barnes maze at week 1 post-MCAO. (C) distance moved on an open field, latency to escape, number of incorrect entries on Barnes maze, and Nest building assessment at week 2 post-MCAO. (D) percentage tissue loss and infarct (red dotted line) Iba1 and GFAP positive counts in peri-infarct region (red boxes). Data presented as mean \pm SEM. $N = 8-10$ /gp. Data were analyzed using the Unpaired t-test with Welch's correction. NDS analyzed by Mann Whitney test and presented as a Median with an interquartile range. ****** $p < 0.01$.

Supplementary Material 4: Suppl. Figure 4: percentage IL-6 and expression increased at 24 h in both sexes after stroke by flow cytometry. (A) Representative dot plots showing the gating strategy for Ly6C^{hi} monocytes and neutrophils. (B) Percentage IL-6 in sham and 24 h after MCAO. (C) MFI IL-6 in sham and 24 h after MCAO. Data presented as mean ± SEM. *n* = 3–4/gp Two-way ANOVA with Tukey's multiple comparisons test. **p* < 0.05; ***p* < 0.01, ****p* < 0.001.

Supplementary Material 5: Suppl. Figure 5: systemic LBP and IL-6 levels at day 30 in males and day 14 in females after stroke. (A) Plasma of LBP and IL-6 levels at day 30 post-MCAO in males. (B) Plasma of LBP and IL-6 levels at day 30 post-MCAO in females at day 14 post-MCAO. Data presented as mean ± SEM. *n* = 6–10/gp. Two group comparisons were analyzed by Unpaired t-test with Welch's correction and three group data were analyzed by Ordinary one-way ANOVA with Tukey's multiple comparisons. **p* < 0.05; ***p* < 0.01, ****p* < 0.001.

Acknowledgements

Not applicable.

Author contributions

AC conceptualized the study, designed, and performed the surgeries, oversaw the experiments, reviewed the data, and wrote and analyzed the manuscript. CH, DN, and KM performed behavioral experiments, IHC, and flow cytometry, and analyzed and drafted the manuscript. CT assisted with the IHC and analysis. All authors have read and approved the manuscript.

Funding

This work was funded by the National Institute of Neurological Disorders and Stroke 1R01NS128412-01A1 to AC.

Data availability

All the data supporting the findings of this study are available on request from the corresponding author.

Declarations

Ethical approval

Animal procedures were approved by the Animal Welfare Committee at the University of Texas Health Science Center in Houston, TX, USA.

Consent for publication

Not applicable.

Competing interests

The authors declare no competing interests.

Received: 20 August 2024 / Accepted: 1 February 2025

Published online: 26 February 2025

References

- Zhu H, Hu S, Li Y, Sun Y, Xiong X, Hu X et al. Interleukins and ischemic stroke. *Front Immunol*. 2022;13.
- Jenny NS, Callas PW, Judd SE, McClure LA, Kissela B, Zakai NA, et al. Inflammatory cytokines and ischemic stroke risk: the REGARDS cohort. *Neurology*. 2019;92(20):e2375–84.
- Hotter B, Hoffmann S, Ulm L, Meisel C, Fiebach JB, Meisel A. IL-6 plasma levels correlate with cerebral perfusion deficits and infarct sizes in Stroke patients without Associated infections. *Front Neurol*. 2019;10:83.
- Montgomery A, Tam F, Gursche C, Cheneval C, Besler K, Enns W, et al. Overlapping and distinct biological effects of IL-6 classic and trans-signaling in vascular endothelial cells. *Am J Physiol Cell Physiol*. 2021;320(4):C554–65.
- Garbers C, Rose-John S. Dissecting Interleukin-6 classic- and trans-signaling in inflammation and Cancer. *Methods Mol Biol*. 2018;1725:127–40.
- Scheller J, Chalaris A, Schmidt-Arras D, Rose-John S. The pro- and anti-inflammatory properties of the cytokine interleukin-6. *Biochim Biophys Acta*. 2011;1813(5):878–88.
- Reeh H, Rudolph N, Billing U, Christen H, Streif S, Bullinger E, et al. Response to IL-6 trans- and IL-6 classic signalling is determined by the ratio of the IL-6 receptor alpha to gp130 expression: fusing experimental insights and dynamic modelling. *Cell Commun Signal*. 2019;17(1):46.
- Papadopoulos A, Palaiopoulos K, Bjorkbacka H, Peters A, de Lemos JA, Seshadri S, et al. Circulating Interleukin-6 levels and incident ischemic stroke: a systematic review and Meta-analysis of prospective studies. *Neurology*. 2022;98(10):e1002–12.
- Suzuki S, Tanaka K, Suzuki N. Ambivalent aspects of interleukin-6 in cerebral ischemia: inflammatory versus neurotrophic aspects. *J Cereb Blood Flow Metab*. 2009;29(3):464–79.
- Gertz K, Kronenberg G, Kalin RE, Baldinger T, Werner C, Balkaya M, et al. Essential role of interleukin-6 in post-stroke angiogenesis. *Brain*. 2012;135(Pt 6):1964–80.
- Loddick SA, Turnbull AV, Rothwell NJ. Cerebral interleukin-6 is neuroprotective during permanent focal cerebral ischemia in the rat. *J Cereb Blood Flow Metab*. 1998;18(2):176–9.
- Li X, Wu X, Chen X, Peng S, Chen S, Zhou G, et al. Selective blockade of interleukin 6 trans-signaling depresses atrial fibrillation. *Heart Rhythm*. 2023;20(12):1759–70.
- Schuett H, Oestreich R, Waetzig GH, Annema W, Luchtfeld M, Hillmer A, et al. Transsignaling of interleukin-6 crucially contributes to atherosclerosis in mice. *Arterioscler Thromb Vasc Biol*. 2012;32(2):281–90.
- Burton MD, Sparkman NL, Johnson RW. Inhibition of interleukin-6 trans-signaling in the brain facilitates recovery from lipopolysaccharide-induced sickness behavior. *J Neuroinflammation*. 2011;8:54.
- Burton MD, Rytch JL, Freund GG, Johnson RW. Central inhibition of interleukin-6 trans-signaling during peripheral infection reduced neuroinflammation and sickness in aged mice. *Brain Behav Immun*. 2013;30:66–72.
- Madsen TE, Khoury JC, Leppert M, Alwell K, Moomaw CJ, Sucharew H, et al. Temporal trends in Stroke Incidence over Time by Sex and Age in the GCNKSS. *Stroke*. 2020;51(4):1070–6.
- Ekker MS, Verhoeven JI, Vaartjes I, van Nieuwenhuizen KM, Klijn CJM, de Leeuw FE. Stroke incidence in young adults according to age, subtype, sex, and time trends. *Neurology*. 2019;92(21):e2444–54.
- Bejot Y, Daubail B, Jacquin A, Durier J, Osseby GV, Rouaud O, et al. Trends in the incidence of ischaemic stroke in young adults between 1985 and 2011: the Dijon Stroke Registry. *J Neurol Neurosurg Psychiatry*. 2014;85(5):509–13.
- Das SK, Banerjee TK, Biswas A, Roy T, Raut DK, Mukherjee CS, et al. A prospective community-based study of stroke in Kolkata, India. *Stroke*. 2007;38(3):906–10.
- Chauhan A, Al Mamun A, Spiegel G, Harris N, Zhu L, McCullough LD. Splenectomy protects aged mice from injury after experimental stroke. *Neurobiol Aging*. 2018;61:102–11.
- Verma R, Ritzel RM, Harris NM, Lee J, Kim T, Pandi G, et al. Inhibition of mir-141-3p ameliorates the negative effects of Poststroke Social isolation in aged mice. *Stroke*. 2018;49(7):1701–7.
- Liu F, Yuan R, Benashski SE, McCullough LD. Changes in experimental stroke outcome across the life span. *J Cereb Blood Flow Metab*. 2009;29(4):792–802.
- Manwani B, Liu F, Xu Y, Persky R, Li J, McCullough LD. Functional recovery in aging mice after experimental stroke. *Brain Behav Immun*. 2011;25(8):1689–700.
- Deacon RM. Assessing nest building in mice. *Nat Protoc*. 2006;1(3):1117–9.
- Hudobenko J, Ganesh BP, Jiang J, Mohan EC, Lee S, Sheth S, et al. Growth differentiation factor-11 supplementation improves survival and promotes recovery after ischemic stroke in aged mice. *Aging*. 2020;12(9):8049–66.
- Labonte B, Engmann O, Purushothaman I, Menard C, Wang J, Tan C, et al. Sex-specific transcriptional signatures in human depression. *Nat Med*. 2017;23(9):1102–11.
- Nguyen JN, Mohan EC, Pandya G, Ali U, Tan C, Kofler JK, et al. CD13 facilitates immune cell migration and aggravates acute injury but promotes chronic post-stroke recovery. *J Neuroinflammation*. 2023;20(1):232.
- Liu F, Schafer DP, McCullough LD. TTC, fluoro-Jade B and NeuN staining confirm evolving phases of infarction induced by middle cerebral artery occlusion. *J Neurosci Methods*. 2009;179(1):1–8.
- Lee MJ, Lee JK, Choi JW, Lee CS, Sim JH, Cho CH, et al. Interleukin-6 induces S100A9 expression in colonic epithelial cells through STAT3 activation in experimental ulcerative colitis. *PLoS ONE*. 2012;7(9):e38801.
- Robinson R, Srinivasan M, Shanmugam A, Ward A, Ganapathy V, Bloom J, et al. Interleukin-6 trans-signaling inhibition prevents oxidative stress in a mouse model of early diabetic retinopathy. *Redox Biol*. 2020;34:101574.

31. Plamondon H, Khan S. Characterization of anxiety and habituation profile following global ischemia in rats. *Physiol Behav.* 2005;84(4):543–52.
32. Milot MR, Plamondon H. Time-dependent effects of global cerebral ischemia on anxiety, locomotion, and habituation in rats. *Behav Brain Res.* 2009;200(1):173–80.
33. Hatakeyama M, Ninomiya I, Kanazawa M. Angiogenesis and neuronal remodeling after ischemic stroke. *Neural Regen Res.* 2020;15(1):16–9.
34. Donegan JJ, Girotti M, Weinberg MS, Morilak DA. A novel role for brain interleukin-6: facilitation of cognitive flexibility in rat orbitofrontal cortex. *J Neurosci.* 2014;34(3):953–62.
35. Bobbo VC, Engel DF, Jara CP, Mendes NF, Haddad-Tovoli R, Prado TP, et al. Interleukin-6 actions in the hypothalamus protects against obesity and is involved in the regulation of neurogenesis. *J Neuroinflammation.* 2021;18(1):192.
36. Jones SA, Richards PJ, Scheller J, Rose-John S. IL-6 transsignaling: the in vivo consequences. *J Interferon Cytokine Res.* 2005;25(5):241–53.
37. McFarland-Mancini MM, Funk HM, Paluch AM, Zhou M, Giridhar PV, Mercer CA, et al. Differences in wound healing in mice with deficiency of IL-6 versus IL-6 receptor. *J Immunol.* 2010;184(12):7219–28.
38. Tschakowsky K, Hedwig-Geissing M, Schmidt J, Braun GG. Lipopolysaccharide-binding protein for monitoring of postoperative sepsis: complementary to C-reactive protein or redundant? *PLoS ONE.* 2011;6(8):e23615.
39. Ritzel RM, Patel AR, Grenier JM, Crapser J, Verma R, Jellison ER, et al. Functional differences between microglia and monocytes after ischemic stroke. *J Neuroinflammation.* 2015;12:106.
40. Xu H, Liu J, Niu M, Song S, Wei L, Chen G, et al. Soluble IL-6R-mediated IL-6 trans-signaling activation contributes to the pathological development of psoriasis. *J Mol Med (Berl).* 2021;99(7):1009–20.
41. Rodriguez-Hernandez MA, Baena-Bustos M, Carneros D, Zurita-Palomo C, Munoz-Pinillos P, Millan J, et al. Targeting IL-6 trans-signaling by sgp130Fc attenuates severity in SARS-CoV-2-infected mice and reduces endotheliopathy. *EBioMedicine.* 2024;103:105132.
42. Schreiber S, Aden K, Bernardes JP, Conrad C, Tran F, Hoper H, et al. Therapeutic Interleukin-6 trans-signaling inhibition by Olamkcept (sgp130Fc) in patients with active inflammatory bowel disease. *Gastroenterology.* 2021;160(7):2354–66. e11.
43. Gronhoj MH, Clausen BH, Fenger CD, Lambertsen KL, Finsen B. Beneficial potential of intravenously administered IL-6 in improving outcome after murine experimental stroke. *Brain Behav Immun.* 2017;65:296–311.
44. Gong H, Li Z, Huang G, Mo X. Effects of peripheral blood cells on ischemic stroke: Greater immune response or systemic inflammation? *Heliyon.* 2024;10(11):e32171.
45. Mullberg J, Schooltink H, Stoyan T, Gunther M, Graeve L, Buse G, et al. The soluble interleukin-6 receptor is generated by shedding. *Eur J Immunol.* 1993;23(2):473–80.
46. Mullberg J, Schooltink H, Stoyan T, Heinrich PC, Rose-John S. Protein kinase C activity is rate limiting for shedding of the interleukin-6 receptor. *Biochem Biophys Res Commun.* 1992;189(2):794–800.
47. Jostock T, Mullberg J, Ozbek S, Atreya R, Blinn G, Voltz N, et al. Soluble gp130 is the natural inhibitor of soluble interleukin-6 receptor transsignaling responses. *Eur J Biochem.* 2001;268(1):160–7.
48. Warach S, Latour LL. Evidence of reperfusion injury, exacerbated by thrombolytic therapy, in human focal brain ischemia using a novel imaging marker of early blood-brain barrier disruption. *Stroke.* 2004;35(11 Suppl 1):2659–61.
49. Zhang M, Liu Q, Meng H, Duan H, Liu X, Wu J, et al. Ischemia-reperfusion injury: molecular mechanisms and therapeutic targets. *Signal Transduct Target Ther.* 2024;9(1):12.
50. Mostajeran M, Edvinsson L, Ahnstedt H, Arkelius K, Ansar S. Repair-related molecular changes during recovery phase of ischemic stroke in female rats. *BMC Neurosci.* 2022;23(1):23.
51. Lehtonen TK, Helantera H, Solvi C, Wong BBM, Loukola OJ. The role of cognition in nesting. *Philos Trans R Soc Lond B Biol Sci.* 2023;378(1884):20220142.
52. Pekny M, Wilhelmsson U, Tatlisumak T, Pekna M. Astrocyte activation and reactive gliosis—A new target in stroke? *Neurosci Lett.* 2019;689:45–55.
53. Xu S, Lu J, Shao A, Zhang JH, Zhang J. Glial cells: role of the immune response in ischemic stroke. *Front Immunol.* 2020;11:294.
54. Wang Y, Li S, Pan Y, Li H, Parsons MW, Campbell BCV, et al. Tenecteplase versus alteplase in acute ischaemic cerebrovascular events (TRACE-2): a phase 3, multicentre, open-label, randomised controlled, non-inferiority trial. *Lancet.* 2023;401(10377):645–54.
55. Sakata H, Narasimhan P, Niizuma K, Maier CM, Wakai T, Chan PH. Interleukin 6-preconditioned neural stem cells reduce ischaemic injury in stroke mice. *Brain.* 2012;135(Pt 11):3298–310.
56. Feng Q, Wang YI, Yang Y. Neuroprotective effect of interleukin-6 in a rat model of cerebral ischemia. *Exp Ther Med.* 2015;9(5):1695–701.
57. Choi BR, Johnson KR, Maric D, McGavern DB. Monocyte-derived IL-6 programs microglia to rebuild damaged brain vasculature. *Nat Immunol.* 2023;24(7):1110–23.
58. Getts DR, Terry RL, Getts MT, Muller M, Rana S, Shrestha B, et al. Ly6c+ inflammatory monocytes are microglial precursors recruited in a pathogenic manner in West Nile virus encephalitis. *J Exp Med.* 2008;205(10):2319–37.
59. Ju H, Park KW, Kim I-d, Cave JW, Cho S. Phagocytosis converts infiltrated monocytes to microglia-like phenotype in experimental brain ischemia. *J Neuroinflamm.* 2022;19(1):190.
60. Kopf M, Baumann H, Freer G, Freudenberg M, Lamers M, Kishimoto T, et al. Impaired immune and acute-phase responses in interleukin-6-deficient mice. *Nature.* 1994;368(6469):339–42.
61. Pawar A, Desai RJ, Solomon DH, Santiago Ortiz AJ, Gale S, Bao M, et al. Risk of serious infections in tocilizumab versus other biologic drugs in patients with rheumatoid arthritis: a multidatabase cohort study. *Ann Rheum Dis.* 2019;78(4):456–64.
62. Medeiros R, Castello NA, Cheng D, Kitazawa M, Baglietto-Vargas D, Green KN, et al. alpha7 nicotinic receptor agonist enhances cognition in aged 3xTg-AD mice with robust plaques and tangles. *Am J Pathol.* 2014;184(2):520–9.

Publisher's note

Springer Nature remains neutral with regard to jurisdictional claims in published maps and institutional affiliations.